Dense Granular Flow around a Penetrating Object: Experiment and Hydrodynamic Model

A. Seguin,[1] Y. Bertho,[1] P. Gondret,[1] and J. Crassous[2]

[1]*Univ Paris-Sud, Univ Paris 6, CNRS, Lab FAST, Bâtiment 502, Campus Univ, F-91405 Orsay, France*

[2]*Université Rennes 1, Institut de Physique de Rennes (UMR UR1-CNRS 6251), Bâtiment 11A, Campus de Beaulieu, F-35042 Rennes, France*

(Received 21 February 2011; published 20 July 2011)

We present in this Letter experimental results on the bidimensional flow field around a cylinder penetrating into dense granular matter, together with drag force measurements. A hydrodynamic model based on extended kinetic theory for dense granular flow reproduces well the flow localization close to the cylinder and the corresponding scalings of the drag force, which is found to not depend on velocity, but linearly on the pressure and on the cylinder diameter and weakly on the grain size. Such a regime is found to be valid at a low enough ''granular'' Reynolds number.

DOI: 10.1103/PhysRevLett.107.048001 PACS numbers: 45.70.−n, 45.50.−j

Introduction.—Describing the motion of an obstacle through granular material is the subject of recent and intensive research with applications to industrial configurations but also to biological and earth science, including animal locomotion in sand [1] and impact cratering [2]. While the motion of an object in a simple fluid has been known for a long time, especially in the viscous regime at a low Reynolds number where the fluid flow and the drag force are analytically known due to Stokes's calculation, the motion of an object in granular matter is still an open question. Such a problem is of fundamental interest, along with numerous open questions of statistical physics concerning (for instance) the solid-liquid or jamming transition [3]. Numerous studies have been done concerning the drag force on an object in vertical or horizontal motion in granular matter [4–11]. All these studies find that the drag force does not depend on the velocity at low velocities, and is proportional to the size of the object and to its depth. As in hydrodynamics, the drag force has been shown to depend on the exact shape of the object [8], and also vertical lift forces can develop during horizontal motion [12]. Flow observations of grains have also been reported in chute flow around a fixed cylinder [13,14] and in the two-dimensional situation of a disk pulled at a constant force in a horizontal assembly of disks on a vibrated plate [3]. Fluctuations have been observed in the force or in the velocity with some ''stick-slip'' behavior in some cases [3,6], and the force may depend crucially on the packing volume fraction [3–5]. In this Letter, we investigate, by particle image velocimetry (PIV) measurements, the flow around a cylinder penetrating into a dense granular packing together with force measurements. By a continuum hydrodynamic model based on the kinetic theory extended to dense granular systems, we recover the experimental results of the shear localization close to the cylinder with the view of a ''hot'' cylinder in motion in a viscosity-dependent temperature fluid, together with a good scaling for the drag force.

Experiments.—The experiments consist of a horizontal steel cylinder of diameter 10 mm $\leq d \leq$ 40 mm and length $b = 40$ mm penetrating a rectangular box (0.1 m in height, 0.2 m in width, and 40 mm in thickness) filled with monodisperse millimetric glass beads of diameter 0.5 mm $\leq d_g \leq 4$ mm and density $\rho_g = 2.5 \times 10^3$ kg m^{-3}. The granular medium is prepared by gently stirring the grains with a thin rod and the surface is then flattened using a straightedge. This preparation leads to reproducible results with only small variations. The solid volume fraction is $\Phi \simeq 0.62$, characteristic of a dense granular packing, and the density of the granular medium is thus $\rho = \rho_g \Phi \simeq 1.5 \times 10^3$ kg m^{-3}. The cylinder which is fixed and related to a force transducer by a vertical thin rod, is first above the grain surface and penetrates gradually into the granular packing as the box is raised up by a stepper motor along a vertical translation guide at a constant velocity V_0 ranging from 0.1 to 100 mm s^{-1}. Very careful alignment is used to prevent any blockage of the cylinder during the motion, and the force at the glass walls without grains is totally negligible. The front and rear walls of the box are in glass, allowing visualization of the granular flow around the cylinder. The images taken from a fast video camera (up to 1000 images per second in the full resolution 1024×1024 pixels) are analyzed by PIV software to get the velocity field of the grains. As the camera is fixed in the laboratory frame together with the cylinder, the obtained velocity field shown in Fig. 1 is the velocity of the grains in the frame of reference of the cylinder.

The measured drag force on the cylinder is observed to increase with the depth z_b during its penetration [Fig. 2(a)] with a ratio F/z_b constant to $\pm 10\%$ over the range $d/2 \leq z_b \leq 70$ mm [Fig. 2(b)]. The force is found proportional to the cylinder diameter [Fig. 2(b)] and roughly independent of the velocity [Fig. 2(c)]. We find also a nonlinear dependence of the force on the grain diameter: The force is about constant at a large enough grain size ($d_g \gtrsim 1$ mm) but increases with decreasing grain size ($d_g \lesssim 1$ mm) [Fig. 2(d)].

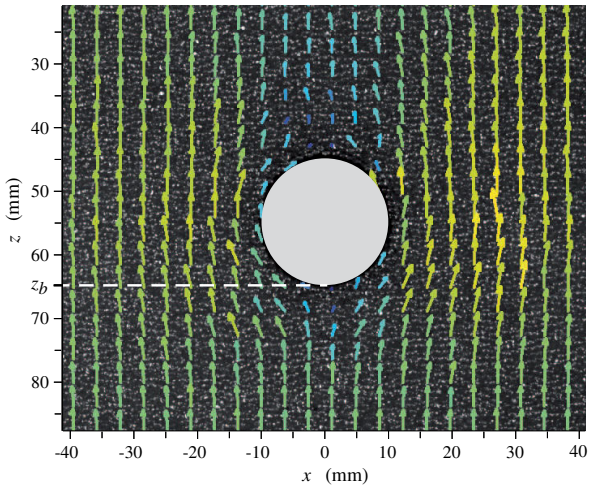

FIG. 1 (color online). Typical instantaneous velocity field obtained by PIV measurements for a cylinder of diameter $d = 20$ mm penetrating into glass beads of diameter $d_g = 1$ mm, at the velocity $V_0 = 5\ \mathrm{mm\,s^{-1}}$, and at the depth $z_b = 65$ mm.

We observe that the grain flow field around the totally immersed cylinder is stationary during the penetration process, meaning that it depends neither on the depth nor on the increasing granular pressure. The velocity field $v(x, z)$ can thus be averaged during each penetration run to extract at each point the mean local velocity $\bar{v}(x, z)$ whose time fluctuations can be related to the local granular temperature T, by $T = \langle (v - \bar{v})^2 \rangle$. We have used cylindrical coordinates (r, θ) where r is the radial distance from the cylinder center and θ is the angle relative to the downward z axis of motion (with thus $\theta = 0$ down): $\mathbf{v}(r, \theta) = v_r(r, \theta)\mathbf{e}_r + v_\theta(r, \theta)\mathbf{e}_\theta$, with the radial and azimuthal components of the velocity v_r and v_θ. As in the classical hydrodynamics situation of a Newtonian fluid, we have checked that v_r and v_θ can be decomposed into cosine and sine functions of θ and radial functions $A_r(r)$ and $A_\theta(r)$: $v_r = -V_0 A_r(r)\cos\theta$ and $v_\theta = V_0 A_\theta(r)\sin\theta$. The radial functions $A_r(r)$ and $A_\theta(r)$ extracted from measurements in the azimuthal range $-\pi/2 < \theta < \pi/2$ are displayed in Fig. 3 and show a strong shear localization when compared to the classical viscous Newtonian case, with exponential variations scaled by the cylinder diameter. At a distance from the cylinder surface larger than about one cylinder diameter ($r \gtrsim 40$ mm in Fig. 3), the grain velocity vanishes. The overshoot of $A_\theta(r)$ expected from mass conservation in the bidimensional configuration is localized close to the cylinder and relaxes to the asymptotic value 1 (no grain flow) with an inflexion point in the present case in contrast with the long-range decay of the Newtonian case at Re $= 0$ (Couette-Poiseuille form).

A typical radial profile of the granular temperature $T(r)$ along the vertical downward line ($\theta = 0$) is displayed in Fig. 4: A domain of roughly constant temperature can be seen around the cylinder with the plateau value T_0 followed by an exponential decrease. The temperature profile is roughly the same for different values of θ and the plateau value T_0 is found to vary with the penetration velocity as $T_0 \sim V_0^2$ (see inset of Fig. 4).

Hydrodynamic model.—The granular mean velocity and its fluctuation show important spatial variations. The strong localization of the granular flow that we observe is a rather usual feature of disordered matter where shear bands are commonly observed (see [15] for a recent review). We show here that the observed shear bands may be understood using a hydrodynamic description. The starting points are that local momentum and energy balance equations, written as [16]

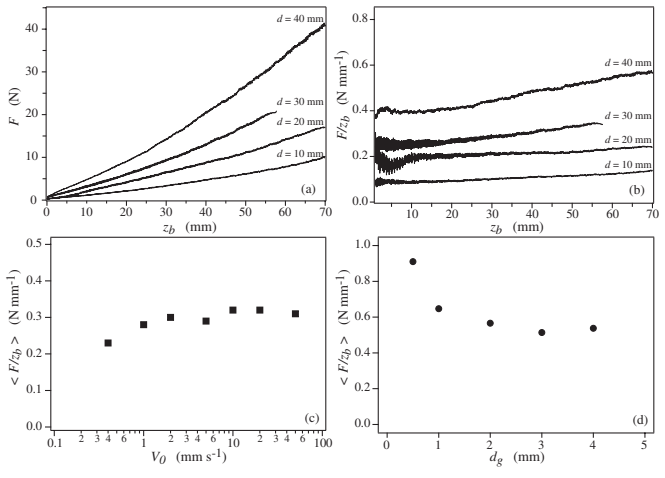

FIG. 2. (a) Drag force F on the cylinder as a function of the penetration depth z_b for different cylinder diameters from $d = 10$ mm to $d = 40$ mm ($d_g = 1$ mm, $V_0 = 5\ \mathrm{mm\,s^{-1}}$). (b) F/z_b for the same data as (a). (c) $\langle F/z_b \rangle$ as a function of V_0 ($d = 20$ mm, $d_g = 1$ mm) and (d) as a function of d_g ($d = 40$ mm, $V_0 = 5\ \mathrm{mm\,s^{-1}}$). $\langle F/z_b \rangle$ is the average of F/z_b over the range $d/2 \le z_b \le 70$ mm.

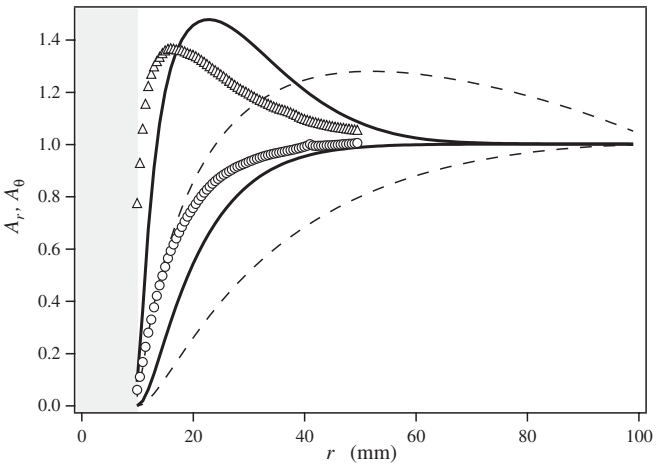

FIG. 3. Radial velocity functions A_r and A_θ as a function of the distance r from the cylinder. Experimental data (circles) A_r and (triangles) A_θ from PIV measurements, (solid lines) profiles obtained by using granular kinetic theory, and (dashed lines) classical Newtonian profiles.

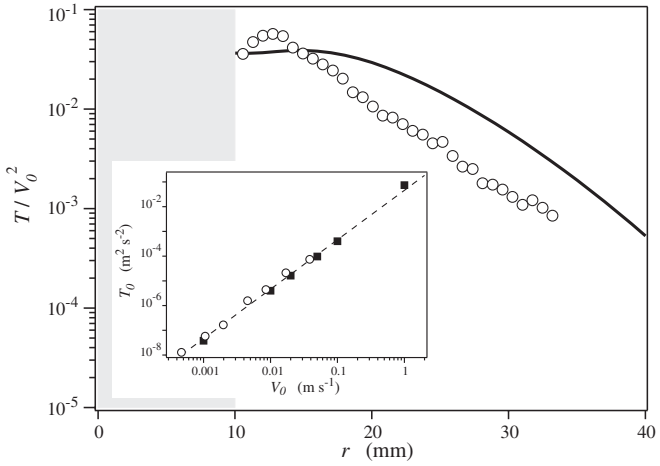

FIG. 4. (circles) Experimental and (solid line) theoretical profiles of the granular temperature T/V_0^2 as a function of the distance r from the cylinder, for $\theta = 0$. Inset: (circles) experimental and (squares) theoretical plateau temperature T_0 as a function of V_0, and (dashed line) power fit of the data of the form $T_0 \propto V_0^2$.

$$\rho \frac{d\mathbf{v}}{dt} = \boldsymbol{\nabla} \cdot \sigma, \tag{1}$$

$$\rho \frac{dT}{dt} = \sigma{:}\kappa - \boldsymbol{\nabla} \cdot \mathbf{q} - \varepsilon T, \tag{2}$$

where ρ is the effective fluid density, σ the stress tensor, $\mathbf{q}$ the heat flux, κ the velocity-gradient tensor, and ε the temperature-loss coefficient. The stress and the heat flux are related to the velocity, temperature, and pressure by phenomenological equations. The choice of these phenomenological equations to describe granular matter is still a matter of debate. If momentum transfer and dissipation occur during binary collisions between grains, granular material may be treated using an inelastic gas theory [17], leading to a Newtonian fluid with $\sigma = -P\mathbb{I} + 2\eta\kappa$, and Fourier's law $\mathbf{q} = -\lambda\boldsymbol{\nabla}T$ for the heat flux. Here P is the pressure, η the viscosity, λ the thermal conductivity, and $\mathbb{I}$ the unit tensor. For simplicity, we neglect dissipation and heat transport associated with compressibility and we treat granular matter as an incompressible fluid as experimentally observed. *A priori*, in a dense granular flow, nonbinary collisions cannot be neglected and transport coefficients from inelastic gas theory [17] are no longer valid. By analogy with glassy materials, modification of the viscosity divergence near jamming has been suggested [18]. Numerical simulations of 2D granular materials seem then to show viscosity divergence at packing fractions lower than random close packing [16,19]. Since in our experiment, most of the shear is located in a region of high velocity fluctuations, we are not very close to random close packing, and therefore we use the Enskog expressions of the phenomenological coefficients [17]:

$$P = \rho_g T f_P(\Phi), \tag{3}$$

$$\eta = \rho_g d_g \sqrt{T} f_\eta(\Phi), \tag{4}$$

$$\lambda = \rho_g d_g \sqrt{T} f_\lambda(\Phi), \tag{5}$$

$$\varepsilon = (1 - e^2) \frac{\rho_g \sqrt{T}}{d_g} f_\varepsilon(\Phi), \tag{6}$$

where f_P, f_η, f_λ, and f_ε are nondimensional functions of the solid volume fraction Φ, and e is the velocity restitution coefficient. For $\Phi \gtrsim 0.5$, those functions vary with the same dependence on Φ [17]. So we have $\eta(P, T) \simeq \eta_0 \times (Pd_g/\sqrt{T})$, $\lambda(P, T) \simeq \lambda_0 \times (Pd_g/\sqrt{T})$, and $\varepsilon(P, T) \simeq \varepsilon_0 \times (P/d_g\sqrt{T})$, with $\eta_0 \simeq 0.28$, $\lambda_0 \simeq 1.06$, and $\varepsilon_0 \simeq 0.34$ [17] with a standard value $e \simeq 0.9$ for glass beads. Those expressions of transport and dissipation coefficients emphasize the fact that Φ is not fixed in our experiment but may vary slightly from point to point in response to pressure and granular temperature variations.

The momentum and heat equations (1) and (2) with $T - P$ dependent transport coefficients are solved numerically for the stationary flow around a cylinder located at the center of a $L \times L$ square box. The momentum equation is solved using a Lattice-Bolzmann solver (BGK based D2Q9 model) with nonslip velocity conditions on the cylinder, constant pressure P_0 at the top of the square box, and constant upward velocity $\mathbf{V}_0$ on the other sides. The heat equation is solved using a finite difference scheme with the condition $\mathbf{e}_r \cdot \boldsymbol{\nabla}T = 0$ on the cylinder and $T = 0$ on the sides of the square box in agreement with experimental findings. The transport coefficients are taken initially homogeneous in the box and the velocity field is first computed by solving the momentum equation with these initial values. From the obtained pressure and velocity fields, the source of heat $\sigma{:}\,\kappa$ is calculated and the heat equation is then computed, leading to a new temperature field. With the new corresponding fields of transport coefficients as inputs, the momentum equation and then heat equation are solved again and so on. After a few iterations, stationary temperature, pressure, and velocity fields which verify (1) and (2) are obtained. In order to prevent numerical instabilities, viscosity is kept in a finite range. The stationary solution is not sensitive to the initial guess of temperature, or to the cutoff of viscosity. Other boundary conditions at the cylinder (the partial velocity slip and Robin condition $dT/dr \propto T$ for the temperature) do not change significantly the velocity and temperature fields.

Results.—Our hydrodynamic model reproduces quite well the experimental features observed in the experiments. The radial temperature profile shows the same shape as in the experiments, with a plateau of high temperature T_0 close to the cylinder followed by an exponential decrease (Fig. 4). The temperature plateau is also found to be proportional to V_0^2 as in the experiments (see inset of Fig. 4). The computed velocity field is found close to the experimental one as shown in Fig. 3 with a shear

localization near the cylinder, and is far from the classical Newtonian case. This shear localization may then be interpreted as a consequence of the strong coupling between viscosity and temperature. At a given pressure the viscosity varies as $\eta \sim 1/\sqrt{T}$. So, at a given viscous shear stress σ_v, the production of heat is proportional to $\sigma_v^2/\eta \sim \sqrt{T}$. This mechanism creates a self-lubricating layer of low viscosity near the cylinder.

The drag force on the cylinder is calculated by integrating the stresses on the disk, taking into account both the ''pressure'' term (from normal stresses) and ''viscosity'' term (from shear stresses). If these two terms are equal in the Newtonian case, the pressure term is here about twice the viscosity term. The total calculated drag force is found to be independent of the velocity, proportional to the cylinder diameter and to the pressure, in agreement with the experimental observations by considering that pressure is proportional to depth. That dependence may be understood in the hydrodynamical model by considering a ''granular'' Reynolds number $\mathrm{Re} = \rho V_0 d/\eta_w$ based on the viscosity η_w near the cylinder. We have checked that all these previous findings correspond to a low Reynolds number regime ($\mathrm{Re} \lesssim 1$). In low Re hydrodynamics, one expects that the force scales as $\eta_w \times V_0$, and then varies here linearly with the pressure, and independently of the velocity as η_w is proportional to the pressure and to $T_0^{-1/2}$ thus to V_0^{-1}. We also found numerically the same nonlinear variation of the drag force with the grain size as in the experiments. Note that this variation is hard to infer simply from the set of equations. When $\mathrm{Re} \gtrsim 1$, the velocity field no longer exhibits up- or downstream symmetry, and the pressure and temperature profiles are also different from the $\mathrm{Re} \lesssim 1$ case.

Concluding remarks.—We have investigated experimentally the penetration of a cylinder at a constant velocity inside a dense granular packing with both force and velocity field measurements, and we have modeled this problem by a continuum hydrodynamic approach. The finding of a strong shear localization close to the cylinder can be viewed by the coupling between viscosity and temperature in the problem of a self-heated cylinder. The localization of the flow near a sedimenting hot sphere has indeed already been reported in classical fluids with temperature dependent viscosity [20]. Such a shear localization has been seen also for a sphere sedimenting in a non-Newtonian fluid with shear thinning behavior [21]. The experimental findings of a force regime independent of velocity and proportional to the depth and to the cylinder diameter are recovered by our model based on kinetic theory adapted for dense granular systems, and have been shown to correspond to a hydrodynamic regime of a low granular Reynolds number. Other models exist for dense granular flows such as the one based on a local rheology with a friction coefficient $\mu(I)$ depending on a nondimensional shear rate I [22]. Such models may also lead to the observed flow localization since it corresponds to viscoplastic or shear thinning behavior. Another issue to explore would be the different force values measured in the plunging and the withdrawal situations [4,10], and what role is played by gravity and the boundary conditions (bottom wall vs free surface). In addition, the force scaling is expected to change in a higher Reynolds regime from a ''viscous'' scaling to an ''inertial'' scaling which may explain the complex force terms measured in impact situations [2,23,24] where the ''granular hydrodynamic'' regime changes certainly from high to low Re during the penetration process. Applications to nonstationary granular flows may also be considered.

We thank J. T. Jenkins, E. Trizac, and E. J. Hinch for stimulating discussions, F. Martinez for his contribution to the experiments, and A. Aubertin for the development of the experimental setup. This work is supported by the ANR project STABINGRAM No. 2010-BLAN-0927-01.

[1] R. D. Maladen *et al.*, Science **325**, 314 (2009).
[2] H. Katsuragi and D. J. Durian, Nature Phys. **3**, 420 (2007).
[3] R. Candelier and O. Dauchot, Phys. Rev. Lett. **103**, 128001 (2009).
[4] M. Schröter *et al.*, Europhys. Lett. **78**, 44 004 (2007).
[5] G. A. Caballero-Robledo and E. Clément, Eur. Phys. J. E **30**, 395 (2009).
[6] I. Albert *et al.*, Phys. Rev. Lett. **84**, 5122 (2000).
[7] R. Albert *et al.*, Phys. Rev. Lett. **82**, 205 (1999).
[8] I. Albert *et al.*, Phys. Rev. E **64**, 061303 (2001).
[9] M. B. Stone *et al.*, Nature (London) **427**, 503 (2004).
[10] G. Hill, S. Yeung, and A. Koehler, Europhys. Lett. **72**, 137 (2005).
[11] F. Zhou, S. G. Advani, and E. R. Wetzel, Phys. Fluids **19**, 013 301 (2007).
[12] Y. Ding, N. Gravish, and D. I. Goldman, Phys. Rev. Lett. **106**, 028001 (2011).
[13] Y. Amarouchene, J. F. Boudet, and H. Kellay, Phys. Rev. Lett. **86**, 4286 (2001).
[14] D. Chehata, R. Zenit, and C. R. Wasgreen, Phys. Fluids **15**, 1622 (2003).
[15] P. Schall and M. van Hecke, Annu. Rev. Fluid Mech. **42**, 67 (2010).
[16] S. Luding, Nonlinearity **22**, R101 (2009).
[17] J. T. Jenkins and S. B. Savage, J. Fluid Mech. **130**, 187 (1983).
[18] L. Bocquet *et al.*, Phys. Rev. E **65**, 011307 (2001).
[19] R. García-Rojo, S. Luding, and J. J. Brey, Phys. Rev. E **74**, 061305 (2006).
[20] A. Ansari and S. Morris, J. Fluid Mech. **159**, 459 (1985).
[21] D. D. Atapattu, R. P. Chhabra, and P. H. T. Uhlherr, J. Non-Newtonian Fluid Mech. **59**, 245 (1995).
[22] P. Jop, Y. Forterre, and O. Pouliquen, Nature (London) **441**, 727 (2006).
[23] D. I. Goldman and P. Umbanhowar, Phys. Rev. E **77**, 021308 (2008).
[24] A. Seguin *et al.*, Europhys. Lett. **88**, 44 002 (2009).